

Characterization of Fluoroelastomer Networks.

I. Infrared Analysis

A. N. THEODORE* and R. O. CARTER III

Ford Research Laboratory, P.O. Box 2053, Dearborn, Michigan 48121

SYNOPSIS

Fluorocarbon compounds based on vinylidene fluoride copolymers and dihydroxy nucleophiles were prepared to determine the network forming structures of the cured materials. Previous attempts to achieve this goal consisted of model compound reactions, of prevulcanization events, and of materials cured under conditions only approaching industrial vulcanization conditions. The proposed structures derived from these studies could be different from the entities that will come in contact with alternate fuels such as methanol/gasoline blends when used in automotive applications. The evolution of the solid-state chemistry during cure and the final network structure needed to be defined. Thus, infrared vibrational spectra for 25- μm thick sections from key stages of processing were recorded. These spectra established directly, for the first time, that bisphenol-AF (BPAF) serves as the crosslinker during cure. Additionally, persistent unsaturation is formed on the elastomer backbone after crosslinking. Curing for extended periods of time produces no observable effect on the network. Furthermore, postcuring reduces residual hydrofluoric acid in the compound and results in two new absorptions at 2851 and 2920 cm^{-1} , indicative of amorphous regions of polyvinylidene fluoride (PVF₂). Although these findings help define the final network structure, there remain uncertainties about the pathway leading to the final structure. The data serve as input to understanding the fracture behavior and long term performance of this class of materials. It also could serve as a starting point for studies dealing with the enhancement of certain fluorocarbon properties such as low temperature behavior. © 1993 John Wiley & Sons, Inc.

INTRODUCTION

Fluoroelastomers, a very stable class of commercial materials, show remarkable resistance to chemical attack and fluid penetration. They are appropriate for use at elevated temperature and in harsh environments such as automotive underhood applications and with oil well "sour gas" mixtures. The copolymers of vinylidene fluoride (VF₂) and hexafluoropropylene (HFP) have received much attention because of availability compared with other commercial monomers. In addition, upon crosslinking the resulting elastomer possesses desirable properties. To improve the final properties of these materials, a variety of bis-nucleophilic agents have

been studied as crosslinkers. However, phase-transfer catalysis (PTC), involving aromatic dihydroxy compounds and "onium" salts, eventually evolved as the crosslinking chemistry of choice. The resulting vulcanizates possess superior properties such as high temperature compression sets.

This material was first generated over 20 years ago; however, the chemical details of the process are not well understood because of the complexity of the product. Early attempts to elucidate the resulting steps occurring during the bis-nucleophilic crosslinking of VF₂/HFP polymer with bisphenol AF (BPAF) were the experiments of Schmiegel.¹ Although the primary reaction system for these studies was the VF₂/HFP dipolymer and the BPAF-onium salt crosslinker, much of pertinent data generated related to model system reactions.

The 19-F NMR data of the reactions of VF₂/HFP with tetrabutylammoniumhydroxide in dimethyl-

* To whom correspondence should be addressed.

formamide indicated that the VF_2 units isolated between HFP units are the most susceptible to dehydrofluorination. A reaction scheme, proposed on the basis of these studies, consisted of dehydrofluorination of the dipolymer, shifting of double bond and reaction of the resulting unsaturated moiety with the nucleophile to produce structure I in Figure 1. However, the above structure was based on the fact that there was very minor crosslinking without incorporation of diphenol. Although the proposed reaction intermediates appear reasonable, they were based on data obtained from model reactions and at the very early stages of the crosslinking process.² The data actually offers very little information as to what takes place after gelation and there is no confirmation of the specific structure of the polymer network.

Subsequently, Velkateswarlu and coworkers³ performed 19-F NMR solution experiments with

VF_2/HFP copolymer and verified most of the findings of Schmiegel. In addition, they studied the release of fluoride ion from the elastomer in the solid state attributable to each of the components of the cure system consisting of calcium hydroxide, magnesium oxide, benzyltriphenylphosphonium chloride (BTTPPCl) and BPAF, as well as certain combinations of these ingredients. The key contribution of this work was the development of certain methodologies in determining chemical events in the solid state. As a result, they proposed $\text{BTTPP}^+ \text{BPAF}^-$ salt as a critical intermediate in the crosslinking reaction originating from the reaction of $\text{Ca}(\text{OH})_2/\text{BTTPPCl}$ or Maglite D (MgO)/BTTPPCl with BPAF. Furthermore, they suggested a reaction mechanism where nucleophilic addition occurs on the $\text{C}(\text{CF}_3)=\text{CH}$ group and not on the $\text{CF}=\text{C}(\text{CF}_3)$ moiety of the diene structure as suggested previously.¹ It was also proposed that nucleophilic attack

Network Structures

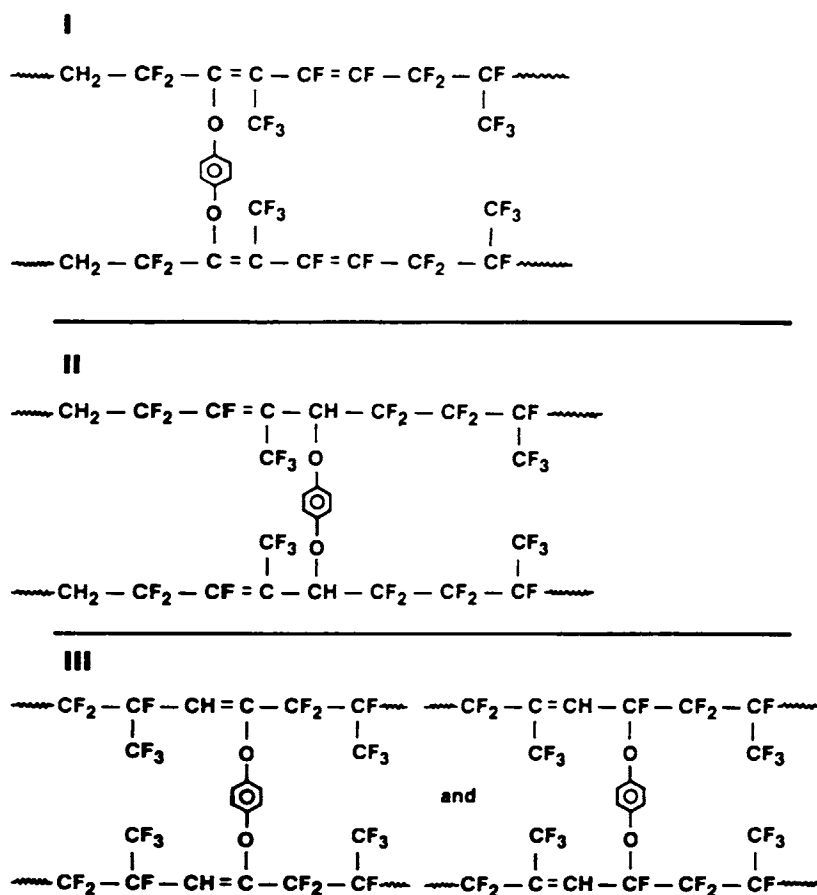


Figure 1 Network structures I, II, and III proposed to represent fluorocarbon A cured with BPAF. $\text{—}\text{O}\text{—}$ is an abbreviation for $\text{—}\text{O}\text{—C—}(\text{CF}_3)_2\text{—O—}$.

occurs with allylic displacement of fluoride. This attack would lead to a new double bond, as shown in structure II of Figure 1. The implications of the above network formation were in agreement with the model reaction data of Apsey et al.⁴

Recently, Arcella et al.⁵ presented a modified reaction mechanism for the crosslinking of VF₂/HFP copolymer with BPAF using relatively standard amounts of BTPPCl as a PTC and Ca(OH)₂ and MgO as acid acceptors and cure activators. It was based on previously described solution investigation using NMR and FTIR data coupled with solid-state vulcanization consisting of oscillating disk rheometry (ODR) and fluoride release measurements. The proposed reaction scheme is consistent with the data generated by these workers with an FTIR experimental set up devised to follow structure evolution during the solid-state crosslinking under conditions close to those employed in commercial vulcanization. It consists of formation of double bond $\text{—C}(\text{CF}_3)=\text{CF—}$ by elimination of "tertiary fluoride," double bond shift catalyzed by the fluoride ion, and nucleophilic addition to the $\text{—CH}=\text{CF—}$ double bond with allylic displacement of fluoride and/or addition/fluoride elimination from the same double bond.

Although the vibrational results obtained with the heated cell are in agreement with previously reported data obtained by infrared analysis performed on solutions,⁶ the prevailing conditions in the heated cell only approximate the conditions of curing in commercial vulcanization operations with respect to pressure. As a result, the final network structure resulting under production conditions could be different from that proposed.⁵

The progress described up to this point sheds light on many of the chemical events that take place during the formation of the network. However, it provides limited understanding of the reaction mechanism attributed to the complexity of the solid-state chemistry of the crosslinking process. A more precise knowledge of the structure of the crosslinked elastomer network is required for the purpose of predicting the performance of these materials in very demanding, harsh environments. Such a knowledge would also be desirable in designing improved network structures by modifying currently available systems.

In this paper, we focus our attention on spectroscopically determining the structure of VF₂/HFP and VF₂/HFP/tetrafluoroethylene (TFE) compounds as they go through the various key steps of the curing process including the postcuring. In contrast to the latest studies that concentrated at best

on approximating the cure process, our approach constitutes a study of the spectra of specimens subjected to real industrial vulcanization conditions. Since the fluoroelastomer network structure resulting from the curing process is far from fully understood, we are attempting to add to the previously reported, pioneering work and to make it more complete. In some experiments data was generated from model compounds in order to support certain points of view.

EXPERIMENTAL

Materials

Fluorocarbon elastomer A is a dipolymer VF₂/HFP obtained from DuPont Co.; Mooney viscosity ML 1 + 10 at 121°C = 22; specific gravity = 1.82; fluorine % = 66; VF₂/HFP mole ratio = 3.5. Fluoroelastomer B is a tripolymer of vinylidene fluoride, hexafluoropropylene, and tetrafluoroethylene (Mooney viscosity ML 1 + 10 at 121°C = 65; specific gravity = 1.85; fluorine % = 68). The gum elastomers were compounded with the other ingredients as received. Curative 20 consists of benzyltriphenylphosphonium chloride (BTPPC) (33% in fluoroelastomer, DuPont Co.) and acts as an accelerator in the curing process. Curative 30 (50% BPAF in fluoroelastomer, DuPont Co.) is the crosslinking moiety in the compound. MgO and Ca(OH)₂ were obtained from C. P. Hall Co. and had purity of 94% minimum. They serve as acid acceptors and cure activators.

Mixing and Molding

Mixing of fluorocarbons A and B with the curatives 20 and 30 and the acid acceptors was performed on a 80 × 180 mm two-roll mill. The mill speed was 3.2 m/min and the gap between the rolls was 0.50 mm. The elastomer was banded on the roll mill and the mixture of ingredients was added slowly over the period of 1 min. Then the mixture was cut continuously at the edges of the roll and placed in the center for 360 s to provide a homogeneous mixture. A typical compound, employed in this study, is shown in Table I (compound A-144). Specimens for these experiments were prepared by compression molding. Previously mixed materials were freshened on a roll mill three or four times and cut to make preforms for molding. Typically the materials were molded at 177°C under 14,000 kg pressure for a fixed time. Sample sheets (150 × 150 × 2 mm) were molded according to ASTM D 3182 and compression

Table I Typical Compound Composition

Fluorocarbon Compound A-144		
Fluoroelastomer A	100.00	phr
Maglite D (MgO)	3.00	phr
Calcium hydroxide [Ca(OH) ₂]	6.00	phr
Curative 20 (BTPPCL)	3.00	phr
Curative 30 (BPAF)	4.00	phr
Fluorocarbon Compound A-91-15		
Fluoroelastomer	100.00	phr
Maglite D (MgO)	4.50	phr
Calcium hydroxide [Ca(OH) ₂]	9.00	phr
Curative 20 (BTPPCL)	4.50	phr
Curative 30 (BPAF)	12.00	phr
Fluorocarbon Compound B-146		
Fluoroelastomer B	100.00	phr
Maglite D (MgO)	3.00	phr
Calcium hydroxide [Ca(OH) ₂]	6.00	phr
Curative 20 (BTPPCL)	3.00	phr
Curative 30 (BPAF)	4.00	phr

set buttons (28-mm diameter \times 13-mm thick) according to ASTM D 395. Postcuring was carried out in an air circulating oven (Blue M) at 200°C for 24 h.

Microtoming of Cylindrical Specimens

Cylindrical specimens were cut from compression set buttons with a 1-cm hole punch. They were placed in a chilled microtome to cut thin film sections 25- μ m thick. The films were thoroughly washed with water and dried before spectral examination.

Spectroscopic Measurements

FTIR spectra were recorded with a Mattson Instruments Galaxy 5020 spectrometer at 8 cm⁻¹ resolution using a sample shuttle. The spectrometer and sample compartment were purged with liquid nitrogen boil off. Cured sections were mounted on masks and scanned 64 times. Similar masks were used on the reference side. Soluble components were scanned as thin films on KBr and powders as KBr pellets. Sixteen scans were used for cast films and pellets.

RESULTS AND DISCUSSION

Prior studies of network structure of cured VF₂/HFP compounds have been based on experimental circumstances that do not completely mimic industrial vulcanization conditions. For example, sample

porosity and the effects of cure under pressure have not been addressed and there is also the issue of the high surface to volume ratios in thin film reactions. Thus, it is necessary to take these reactions to real world conditions to be assured that the reactions occurring in commercial materials are well understood. Hence, the processing of two compounds, A-144 and B-146 prepared using VF₂/HFP and VF₂/HFP/TFE, is reported. The compositions of these two compounds are detailed in Table I. In Figure 2, the cure profiles as measured by ODR are reproduced. Although both materials are compounded identically for nucleophilic crosslinking, the cure profiles indicate that there are some differences in the latency period before rapid changes in the rheometric behavior of the samples. This data was used as a guide in preparing compression molded specimens for infrared analysis. Experiments were designed to monitor the reaction progress before induction of crosslinking, at an early stage of crosslinking and at the later stage of the vulcanization. Also included were samples exposed to curing conditions for extended periods of time and a post-vulcanizing stage (Table II). By elucidating the process at these several stages it is hoped that a more complete and reliable picture of the final material can be established.

By processing the fluoropolymers under realistic conditions and sampling the results by removing a thin section of the product for spectroscopic examination, a picture of the chemistry generated in a commercially processed product is obtained. By and large, the earlier results have been confirmed but some new findings have also presented themselves in the process.

In Figure 3, the infrared spectra of the evolution of crosslinking with time of processing is illustrated for the VF₂/HFP compound. Starting with the cured material, compression molded for 60.0 min [Fig. 3(A)], and proceeding in alphabetical order, spectra representing the samples that were quenched after 15, 4, 2.5, and 1.5 min are illustrated, along with the neat polymer [Fig. 3(F)]. This figure includes the spectral data for the C—H stretching region from 3300 to 2700 cm⁻¹; the C=C stretching region for the unsaturation formed in crosslinking, 1800 to 1650 cm⁻¹; and for the aromatic rings from the crosslinker, 1650 to 1550 cm⁻¹. In the infrared study using a heated cell, the formation of two features track the accumulation of unsaturation in the polymer at 1718 and 1680 cm⁻¹. As earlier, no significant accumulation of unsaturation was observed until the spectrum at 4 min into the vulcanization. However, the spectral intensity at 1680 cm⁻¹ reported herein

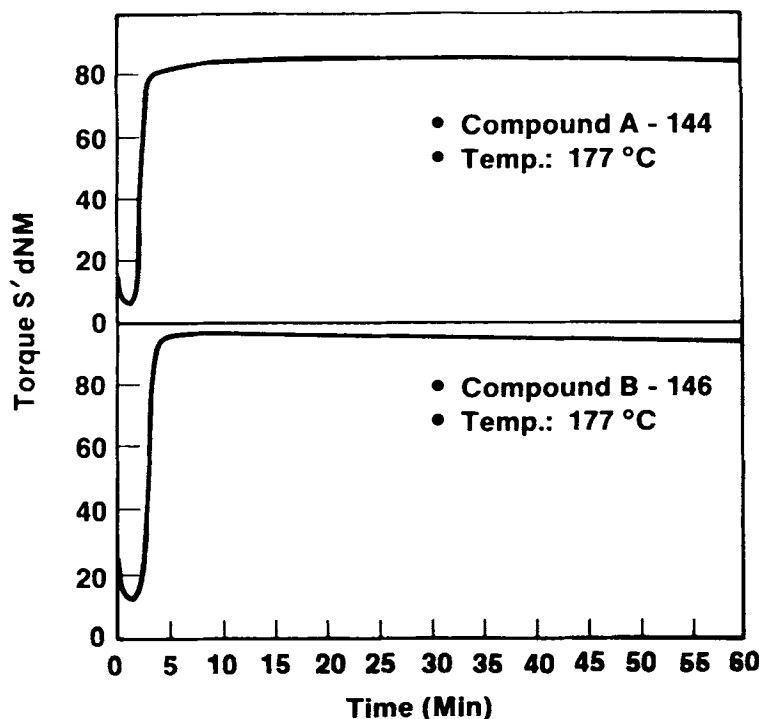


Figure 2 Cure profile of fluorocarbon compound A-144 and B-146 cured at 177°C as followed by ODR. Torque S' , dNm vs. cure time, min.

appears to be greater than that previously reported, when compared to the 1720 cm^{-1} intensity.

The higher frequency of the two apparent ring $\text{C}=\text{C}$ stretching modes attributed to the cross-

Table II Standard Fluorocarbon A at 177°C Taken through the Various Stages of the Cure Process

Compound	Press Cured			Post-cured	
	Temp. (C)	Time (min)	Cure (%)	Temp. (C)	Time (h)
a ^a	177	1.50	0	—	—
b	177	2.50	40	—	—
c	177	4.00	70	—	—
d	177	15.00	100	—	—
Variation in Cure Conditions and Curative Level of Fluorocarbon Compounds					
d ^a	177	15.00	100	—	—
e	177	60.00	100	—	—
f	177	60.00	100	200	24
A-91-15	177	60.00	100	—	—

^a Compounds A-144 (a-f) have the same composition as compound A-144 (Table I).

linker, BPAF, is found initially at 1615 cm^{-1} in the neat material. The feature shifts to a frequency of 1608 cm^{-1} by the time the spectral intensity associated with unsaturation accumulation starts at 4 min into the process. The relative intensity of the neighboring peak at 1595 cm^{-1} appears to decrease with reaction time. These changes may result from the incorporation of the BPAF into the network. If in fact this is the case, then crosslinking with BPAF does not require the accumulation of unsaturation but proceeds prior to such an accumulation as indicated by this data obtained from the solid-state process.

In Figure 4, the absence of crosslinker on the time evolution of the unsaturation is documented. In the first minute and a half the only evidence of unsaturation is seen as a broad feature centered at 1650 cm^{-1} , and trace of evidence for a band at 1718 and 1680 cm^{-1} [Fig. 4(D)]. By approximately 3 min into the reaction the feature associated with unsaturation has become even broader and more intense with a distinct band at 1718 cm^{-1} [Fig. 4(C)]. At 6 min [Fig. 4(B)], in the absence of BPAF, the 1718 cm^{-1} band is clearly evident but even at 15 min [Fig. 4(A)], there is only weak indication of a 1680 cm^{-1} feature. The product of the BPAF-free experiment was vulcanized as has been recorded previously,¹ and

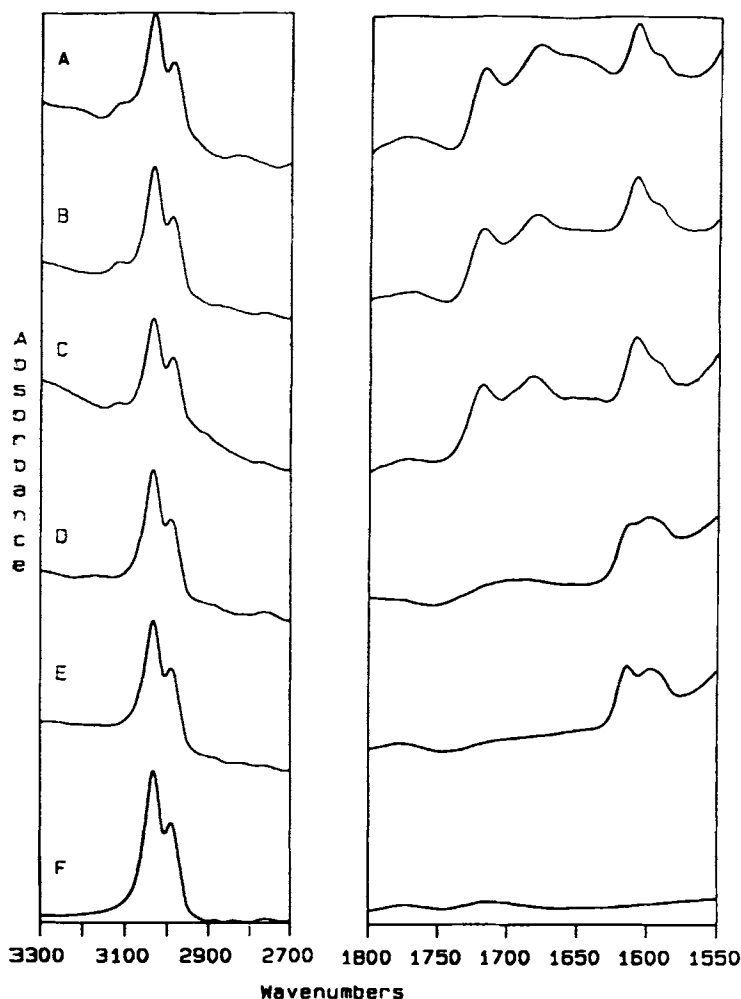


Figure 3 Infrared spectra from 25- μm thick sections in the C—H stretching region, 3300 to 2700 cm^{-1} ; and C=C stretching region, 1800–1550 cm^{-1} ; for the A-144 compound cured for 60 min cure, A; 15 min, B; 4 min, C; 2.5 min, D; 1.5 min, E; and neat polymer, F.

the color of the product is the same dark brown as observed in the presence of the BPAF. Thus, there is a different type of crosslinking taking place (Table III).

In the presence of three times the BPAF and 1½ times the BTPPC the 1718 cm^{-1} intensity is approximately constant but the 1680 cm^{-1} band grows with increased crosslinker [Fig. 5(B) vs. (C)]. When the intensity of Figure 5(B) is scaled for the increase in BTPPC, the overall intensity in the 1750 to 1550 cm^{-1} region overlaps with Figure 5(C) with the exception that the 1680 and 1610 cm^{-1} bands are increased and there is a decrease in the 1600 cm^{-1} region. In the absence of crosslinker [Fig. 5(A), repeated from 4(A) on the same scale as 5(B) and 5(C)], the unsaturation intensity is increased, especially in the 1600 cm^{-1} domain, but very little

1680 cm^{-1} intensity. In addition to the unsaturated organic group contribution in the 1800–1550 cm^{-1} region, the MgO filler, used as a buffer to HF, also contributes a band at 1640 cm^{-1} because of the presence of water in the crystal lattice that is also observed in the O—H stretching region at 3698 cm^{-1} (spectra not shown). This component would be expected to contribute equally to all three spectra presented in Figure 5.

Supporting these observations concerning the evolution of unsaturation is the C—H stretching region. In the 3300–2700 cm^{-1} region of Figure 3, the presence of unsaturated C—H is present at 3119 cm^{-1} on the high frequency side of the principle C—H stretching band for the cured polymer [Fig. 3(A), cured vs. 3(F), neat polymer]. This feature appears only as the C=C stretches, 1720 and 1680

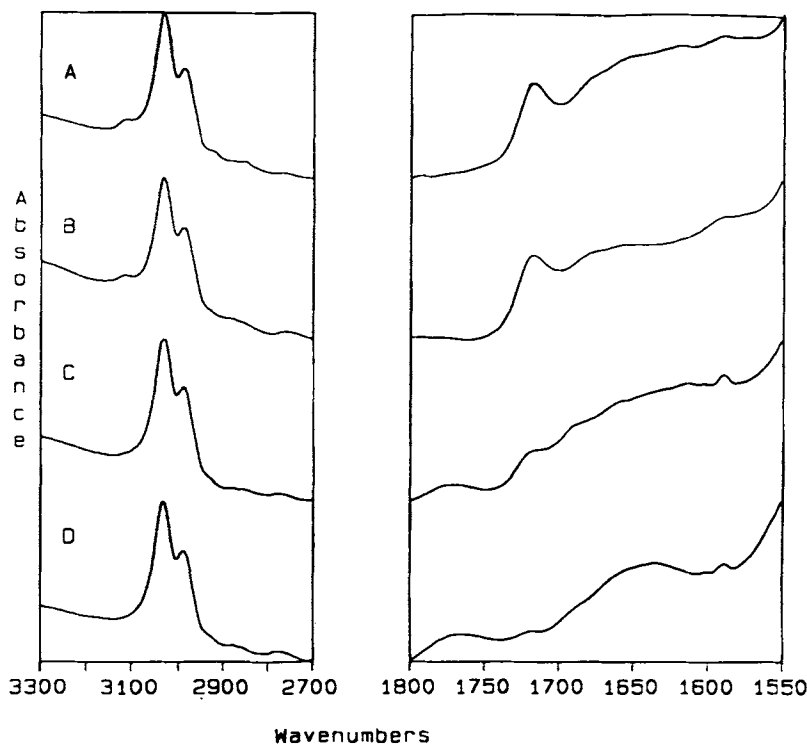


Figure 4 Infrared spectra from 25- μ m thick sections in the C=C stretching region, 1800 to 1550 cm^{-1} : for the A-144 compound less the BPAF crosslinker cured at 177°C for 60 min, A; 6 min, B; 1.5 min, C; and the MgO filler with adsorbed water.

cm^{-1} , appear in spectra [Fig. 3(A-C)]. Thus, unsaturated groups do not appear until after 4 min into the reaction and yet at that point the spectral shift of the BPAF is complete. The appearance of the unsaturated C—H stretch appears in spectra in the presence and the absence of the BPAF, crosslinker, and its associated chemistry [Fig. 4(A-D)].

In addition to the studies of the dipolymer, fully formulated and cured compression set samples were also generated for the tripolymer, which included TFE as well as VF_2 and HFP. In Figure 6, the curing of the B-146 compound is tracked via the C—H stretching and the —C=C— stretching regions

Table III Standard Fluorocarbon Compound without the BPAF Crosslinker

Compound	Solubility	Press Cured	
		Temp. (C)	Time (min)
A-148E	Soluble	177	1.50
A-148E	Partial	177	6.00
A-148E	Partial	177	60.00

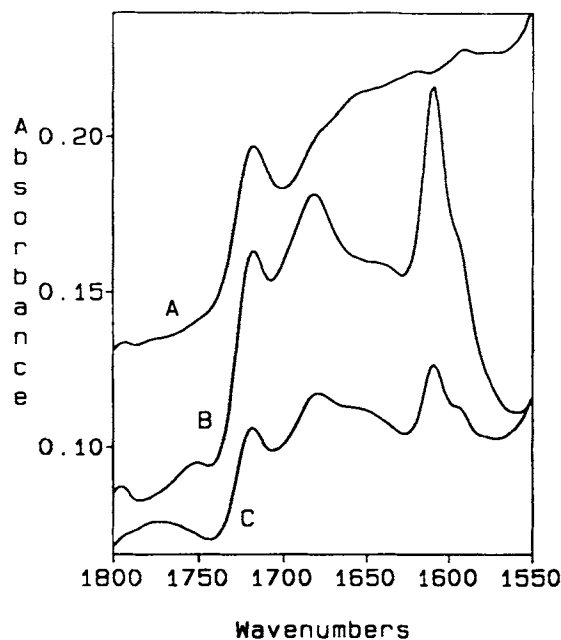


Figure 5 Infrared spectra from 25- μ m thick sections in the C=C stretching region, 1800 to 1550 cm^{-1} : for compound A-144 without crosslinker, A; polymer A compounded with three times the normal amount of BPAF crosslinker; compound A-91-15, B; and compound A-144, C.

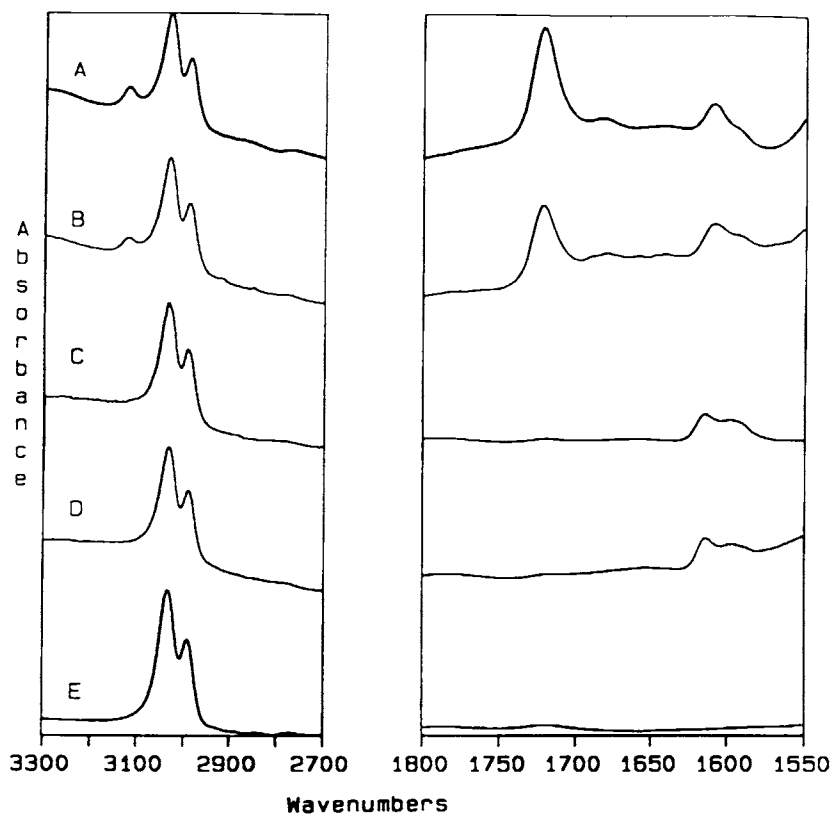


Figure 6 Infrared spectra from 25- μ m thick sections in the C—H stretching region, 3300 to 2700 cm^{-1} ; and C=C stretching region, 1800–1550 cm^{-1} ; for the B-146 compound cured for 12 min cure, A; 6 min, B; 3 min, C; 1.5 min, D; and neat polymer, E.

for 12 min of cure, Figure 6(A), to 6 min of cure, Figure 6(B), to 3 min of cure, Figure 6(C), to 1.5 min cure, Figure 6(D). Included for comparison is the spectrum of the neat polymer, Figure 6(E). Again we observe the same crosslinker absorption frequency shift as above. The shift, which was attributed to the chemical inclusion into the matrix, is completed before there was any evidence for the presence of unsaturated functionality in either spectral region. As before, the ODR trace indicates most of the crosslinking occurs before there is a significant accumulation of vinyl groups.

A comparison of the results for the two polymers in the spectral region from 4000 to 1550 cm^{-1} is presented in Figure 7(B), dipolymer, and 7(D), tri-polymer. Although the spectra are very similar, there are two apparent differences in the spectra of these two materials. The C=C stretching intensity at 1718 cm^{-1} is much stronger in the spectrum of the tri-polymer and the =C—H stretch at 3115 cm^{-1} is somewhat stronger as well. This is probably caused by the change in monomer ratio in the terpolymer. Other than these two differences, the changes upon

curing were similar with respect to the FTIR analysis.

One of the advantages obtained from an *ex situ* experiment is that the effects of posttreatment can be evaluated. The spectra for both formulations A-144 and B-146 after posttreatment at 200°C for 24 h is presented in Figure 7(A) and (C). Again, there is very little change in the spectra upon posttreatment with two exceptions. The band at 3641 cm^{-1} is diminished in the spectra of both materials after posttreatment. This is probably because of the reaction of hydrofluoric acid with calcium hydroxide. The other change, which is also common to the spectra of both materials upon posttreatment, is the appearance of two bands in the C—H stretching region at 2920 and 2851 cm^{-1} .

The assignment of the features that arise or are modified as a result of processing can be understood on the basis of previously developed spectral interpretations of neat materials and small molecules. The two sharp features above 3500 cm^{-1} can easily be identified as $\text{Ca}(\text{OH})_2$ at 3641 cm^{-1} and $\text{MgO} \cdot \text{H}_2\text{O}$ at 3700 cm^{-1} .⁷ The C—H stretches in

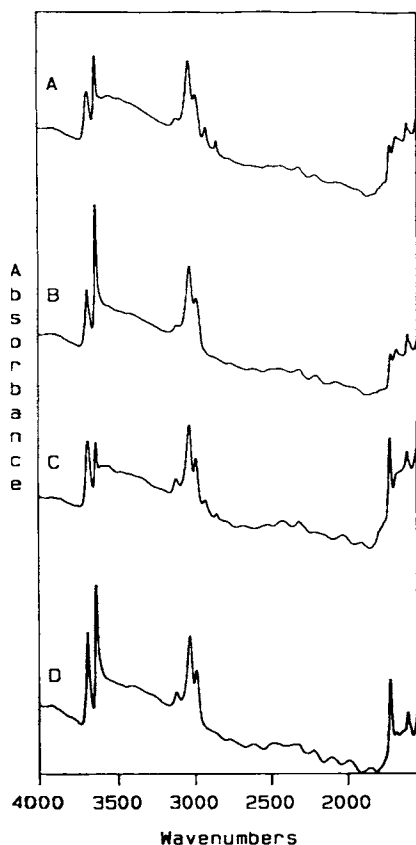


Figure 7 Infrared spectra from 4000 to 1550 cm^{-1} for 25- μm thick sections of compound A-144 post-treated, A; and cured 60 min only, B; and of compound B-146 post-treated, C; and cured 60 min only, D.

the original polymer and all the C—H stretches in the processed materials, with one exception, must be understood in terms of PVF₂ structures. The exception is the 3119 cm^{-1} band that arises after double bonds are formed in the matrix and is attributed to the vinyl carbon stretch, =C—H.⁸ The major bands at about 3000 cm^{-1} in all of the spectra presented here can be attributed to the crystalline forms of PVF₂ as have been identified by Cortili and Zerbi⁹ and Enomoto et al.¹⁰ The two new features at lower frequency, found only upon heating to 200°C, are attributed to amorphous PVF₂.⁹

The —C=C— region from 1720 to 1600 cm^{-1} consists of several types of structures and is thus made up of overlapping bands with a few distinct features. The band at 1718 cm^{-1} has been assigned by several authors to “double bonds carrying a fluorine substituent.”^{11,12} This band has also been attributed to the double-bond stretch of the structure —CF=CH— by others.^{5,13} However, this feature is perhaps better attributed to the structure —CF=CF— or =CF₂ consistent with a wider

set of fluorinated species.^{8,14,15} In support of this is the relative increase in this feature when TFE is included in the polymer, compound B-146.

The band at 1680 cm^{-1} lies in the characteristic frequency ranges for the structures such as $\text{R}_a\text{R}_b\text{C}=\text{CHR}_c$, 1680–1670 cm^{-1} , and $\text{R}_a\text{R}_b\text{C}=\text{CR}_c\text{R}_d$, 1690–1680 cm^{-1} .⁸ The substitution of one fluorine for a proton is expected to raise the C=C stretch only slightly, that is, $\sim 25 \text{ cm}^{-1}$. Even if such a shift is smaller when only one hydrogen is available for substitution, it does not seem likely that the 1680 cm^{-1} feature is associated with the structure, $\text{R}_a\text{R}_b\text{C}=\text{CFR}_c$. However, this band does seem to be present only when crosslinker is included in the compound and seems to vary directly in intensity with the amount of crosslinker present.

The presence of infrared absorption at 1600 cm^{-1} in the crosslinker free compound [Fig. 5(A)] relative to the lack thereof in the presence of crosslinker suggests that there is a different distribution of unsaturated structures especially with respect to conjugated structures. In an earlier study of γ -irradiated PVF₂ and VF/VF₂ distinct features were observed at $\sim 1600 \text{ cm}^{-1}$ that was attributed to conjugated double bonds.¹¹ Thus, the presence of crosslinker seems to inhibit the formation of structures of this nature.

CONCLUSIONS

Fluoroelastomer compounds based on vinylidene fluoride copolymers (VF₂/HFP and VF₂/HFP/TFE) and the BPAF nucleophile were prepared and molded using industrial vulcanization conditions to determine the network structure. As a result, chemical entities, which are expected to be in contact with alternate automotive fuels such as methanol blends, were produced. Although the simplest fluorocarbon elastomers were chosen for this study, crosslinking through phase-transfer catalysis might not be the least complicated processing procedure. To follow chemical events taking place during the solid-state cure, specimens were successfully quenched at the key stages of processing. Cylindrical specimens cut from the molded parts were microtomed into 5–25 micron circular sections for spectroscopic examination.

To identify the main curing events, the complete spectrum of samples representing the key stages of processing were obtained. The findings are outlined below:

1. In the early stage no double bonds are detected by FTIR. However, a small frequency

shift in the ring absorptions of the BPAF is observed.

2. The shift in the ring absorptions of BPAF is associated with crosslinking. This was observed for the first time and correlates well with the ODR data. Further, it appears that crosslinking occurs prior to accumulation of unsaturation. The double-bond absorption at 1680 cm^{-1} also provides a measure of crosslinking. Contrary to previously reported data, the intensity of absorption at 1680 cm^{-1} is higher than that at 1718 cm^{-1} .
3. At 100% cure the intensity of absorption at 1680 cm^{-1} is still higher than that at 1718 cm^{-1} . This trend is not consistent with earlier results but may arise from differences in sample preparation.
4. Maintaining the specimens at the cure conditions for 60 min has no noticeable effect on their spectra.
5. The post-curing treatment results in the decrease of the hydrofluoric acid in the compound and in the formation of amorphous regions of PVF₂.
6. The spectra of dipolymer and terpolymer compounds is similar with the exception of the stronger terpolymer absorptions at 1718 and 3115 cm^{-1} . This is probably caused by the addition of TFE in the terpolymer.

The solid-state data can serve as input in determining the fracture and environmental behavior of these materials. It can also be used as a baseline for those concerned with enhancing certain properties of fluorocarbon materials. Although the network structure has been determined by this approach, there are still uncertainties about the pathway that leads to the final network structure.

The authors would like to thank C. Thomas of the Ford Central Laboratory and his associates for their assistance in this effort.

REFERENCES

1. W. W. Schmieg, *Die Angew. Macromol. Chem.*, **76/77**, 39–65 (1979).
2. S. Smith, in *Preparation, Properties, and Industrial Application of Organic Fluorine Compounds*, R. E. Banks, Ed., E. Horwood Limited, Chichester, Sussex, England, 1982, pp. 235–295.
3. P. Venkaleswarlu, R. A. Guenther, R. E. Kolb, and T. A. Kestner, paper presented at the ACS Rubber Division Meeting, Detroit, MI (1989).
4. G. C. Apsey, R. D. Chambers, M. J. Salisbury, and G. Moggi, *J. Fluorine Chem.*, **40**, 261 (1988).
5. V. Arcella, G. Chiodini, N. DelFanti, and M. Pianca, Paper presented at the ACS Rubber Division Meeting, Detroit, MI (1991).
6. G. Cirillo, G. Chiodini, N. Del Fanti, G. Moggi, and F. Severini, in *Biological Synthetic Polymer Networks*, O. Kramer, Ed., Elsevier Applied Science, London, UK, 1988, p. 255.
7. K. Nakamoto, *Infrared Spectra of Inorganic and Coordination Compounds*, 2nd ed., Wiley-Interscience, New York, 1970, p. 82.
8. L. J. Bellamy, *The Infra-red Spectra of Complex Molecules*, Chapman and Hall, London, 1975, p. 38.
9. G. Cortili and G. Zerbi, *Spectrochim. Acta*, **23A**, 285 (1967).
10. S. Enomoto, Y. Kawai, and M. Sugita, *J. Polym. Sci. A-2*, **6**, 861 (1968).
11. M. Hagiwara, G. Ellinghorst, and D. O. Hummel, *Makromol. Chem.*, **178**, 2913 (1977).
12. H. Kise and H. Ogata, *J. Polymer Sci., Polymer Chem. Ed.*, **21**, 3443 (1983).
13. O. V. Blagodatova, T. B. Zapevalova, and O. V. Kozlova, *Vysokomol. Soedin. B*, **27**, 362 (1985).
14. A. S. Novikov, V. L. Karpov, F. A. Gailil-Ogly, N. A. Slovokhotova, and T. N. Dyumaeva, *Vysokomol. Soedin.*, **2**, 485 (1960).
15. D. G. Weiblen, *The Infrared Spectra of Fluorocarbons*, in *Fluorine Chemistry*, J. H. Simons, ed., Academic Press, New York, 1954, p. 454.

Received September 9, 1992

Accepted September 25, 1992